



Article

# Effect of the Addition of Natural Rice Bran Oil on the Thermal, Mechanical, Morphological and Viscoelastic Properties of Poly(Lactic Acid)

Maria Cristina Righetti <sup>1,\*</sup>, Patrizia Cinelli <sup>1,2</sup>, Norma Mallegni <sup>1</sup>, Carlo Andrea Massa <sup>1</sup>,  
Maria Irakli <sup>3</sup> and Andrea Lazzeri <sup>1,2</sup>

<sup>1</sup> CNR-IPCF, National Research Council—Institute for Chemical and Physical Processes, Via Moruzzi 1, 56124 Pisa, Italy; patrizia.cinelli@unipi.it (P.C.); norma.mallegni@pi.ipcf.cnr.it (N.M.); carloandrea.massa@pi.ipcf.cnr.it (C.A.M.); andrea.lazzeri@unipi.it (A.L.)

<sup>2</sup> Department of Civil and Industrial Engineering, University of Pisa, Largo Lucio Lazzarino 1, 56122 Pisa, Italy

<sup>3</sup> Hellenic Agricultural Organization “Demeter”, Institute of Plant Breeding & Genetic Resources, P.O. Box 60411, GR-57001 Thessaloniki, Greece; irakli@cerealinstitute.gr

\* Correspondence: cristina.righetti@pi.ipcf.cnr.it

Received: 10 April 2019; Accepted: 10 May 2019; Published: 15 May 2019



**Abstract:** For the first time in this study, the utilization of rice bran oil (RBO) as possible totally eco-friendly plasticizer for poly(lactic acid) (PLA) has been investigated. For comparison, the behavior of soybean oil (SO) has also been analyzed. Both oils are not completely miscible with PLA. However, certain compatibility exists between PLA and (i) RBO and (ii) SO, because demixing is not complete. Although not totally miscible, RBO and SO are able to reduce the viscosity of the PLA+RBO and PLA+SO mixtures, which attests that a small amount of RBO or SO can be successfully added to PLA to improve its processability. Additionally, the mechanical properties of the PLA+RBO and PLA+SO mixtures exhibit trends typical of plasticizer-polymer systems. More interestingly, RBO was found to accelerate the growth of PLA  $\alpha'$ -crystals at a low crystallization temperature. This feature is appealing, because the  $\alpha'$ -phase presents lower elastic modulus and higher permeability to water vapor in comparison to the  $\alpha$ -phase, which grows at high temperatures. Thus, this study demonstrates that the addition of RBO to PLA in small percentages is a useful solution for a faster preparation of PLA materials containing mainly the  $\alpha'$ -phase.

**Keywords:** poly(lactic acid); eco-friendly plasticizer; vegetable oils; crystalline form; morphology

## 1. Introduction

Bio-based and/or biodegradable polymers (bioplastics) [1] represent an important alternative to petroleum-derived polymers, which are commonly non-degradable, although in some cases they can be de-polymerized, and thus made sustainable [2]. For this reason, in recent years, bioplastics have gained increasing attention in both the academia and industry. Among them, poly(lactic acid) (PLA) is the biodegradable polymer most present on the market and widely used for packaging purposes. Many properties of PLA, such as strength and stiffness are comparable to those of traditional petroleum-based polymers, whereas a relatively low toughness limits its use [3]. To improve the ductility of PLA materials, different strategies have been adopted, such as for example polymer blending, copolymerization or plasticization [4].

Plasticizers are low-molecular weight non-volatile substances, which are largely used to improve the processability and flexibility of polymers [5]. The main effects of a plasticizer on the properties of a polymeric material are: (i) Decrease in the glass transition temperature ( $T_g$ ), (ii) decrease in the melting temperature ( $T_m$ ), (iii) decrease in the tensile strength, (iv) increase in the elongation at

break, and (*v*) reduction in viscosity [6]. These changes also affect the workability of the materials, because the decrease in  $T_m$  can allow reducing the temperature of processing, and thus also possible polymer degradation.

Ideal plasticizers are miscible or compatible in all proportions with the polymer. Plasticizers reduce the intermolecular forces between the macromolecules, thus increasing the free volume and facilitating the molecular motions [7]. A necessary condition for a good plasticizing action is that the molecular weight of the plasticizer is sufficiently high, so that its mobility is low and possible migration within the polymeric matrix is reduced.

To overcome the toxicity of petroleum-based plasticizers, in recent years, plasticizers for PLA produced from natural sources have been widely utilized and investigated [5,7–22]. This class of plasticizers includes low molecular weight citrate esters [8], oligomeric lactic acid [11], and epoxidized fatty acid esters [12]. In addition, modified vegetable oils (epoxidized or maleinized vegetable oils: Soybean, linseed, palm, cottonseed) have been widely utilized as plasticizers for PLA and PLA-based biocomposites [13–22]. These latter studies fall into the recent and comprehensive interest for plant oils, to be used as an alternative resource for the production of polymers and additive for polymers [23–25].

Unmodified vegetable oils are less utilized as plasticizers for PLA in comparison with functionalized vegetable oils, because in general they are less miscible and/or compatible with PLA, although totally eco-friendly [21]. Some studies have however evidenced that also unmodified oils, such as for example cardanol oil and coconut oil, can act as good plasticizers for PLA [26,27].

For the first time in this study, the utilization of rice bran oil (RBO) as a possible plasticizer for poly(lactic acid) (PLA) has been investigated. For comparison, the behavior of soybean oil (SO) has also been analyzed. Rice (*Oryza sativa* L.) is one of the most important crops worldwide. By-products of rice processing are rice bran and husks, which accounts for 20% of the rough rice [28]. Rice brain, the outer layer of brown rice, serves as a good source of RBO and bioactive compounds like  $\gamma$ -oryzanol, tocopherols, tocotrienols, phytosterols and phenolic compounds, which present an interesting antioxidant activity [29]. The main aim of the present paper is to investigate how the addition of the totally eco-friendly RBO can modify the final thermal, mechanical, morphological and viscoelastic properties of PLA-based materials. This study fits into the widely investigated topic, in general and also by our group [30–34], on the utilization and valorization of agro-food biomass, co-products and by-products, for the production of sustainable polymeric materials, according to the principles of circular economy, in order to favor the production of articles with properties valuable for practical applications, and reduce the cost of the final products.

## 2. Materials and Methods

### 2.1. Materials

Poly(lactic acid) (PLA) derived from natural resources, was 2003D NatureWorks (Minnetonka, MN, USA), grade for thermoforming and extrusion processes, containing 3% of D-lactic acid units [melt flow index (MFI): 6 g/10 min (210 °C, 2.16 kg), nominal average molar mass: 200,000 g/mol].

The refined rice bran oil (RBO) was provided by Hellenic Agricultural Organization “Demeter”, Institute of Plant Breeding and Genetic Resources (Thessaloniki, Greece). The soybean oil (SO) was purchased from Sigma Aldrich (Milan, Italy). The fatty acid composition of the oils, and the concentration of  $\gamma$ -oryzanol, tocotrienols and tocopherols, determined as reported in reference [35], is detailed in Tables 1 and 2, respectively.

**Table 1.** Fatty acid composition of rice bran oil (RBO) and soybean oil (SO).

Fatty Acid	g/100 g Fat RBO	g/100 g Fat SO
C12:0 lauric acid	0.2	-
C14:0 myristic acid	0.4	0.1
C16:0 palmitic acid	16.9	10.6
C16:1 palmitoleic acid	0.2	0.1
C17:0 eptadecanoic acid	-	0.1
C17:1 eptadecenoic acid	-	0.1
C18:0 stearic acid	2.3	4.3
C18:1 oleic acid	41.4	23.9
C18:1 vaccenic acid	0.1	-
C18:2 linoleic acid	34.9	52.6
C18:3 linolenic acid	1.5	7.1
C20:0 arachidic acid	0.4	0.3
C20:1 eicosenoic acid	-	0.2
C22:0 behenic acid	0.2	0.4
C22:1 erucic acid	0.1	-
C24:0 lignoceric acid	0.1	0.1
C24:1 tetracosenoic acid	0.1	-
total	98.8	99.9
Saturated	20.5	15.9
Monounsaturated	41.9	24.3
Polyunsaturated	36.4	59.7

**Table 2.** RBO and SO:  $\gamma$ -oryzanol, tocotrienols and tocopherols content.

	mg/100 mL RBO	mg/100 mL SO
$\gamma$ -oryzanol	81	-
$\delta$ -tocotrienol	3.14	-
$\gamma$ -tocotrienol	10.26	-
$\beta$ -tocotrienol	0.37	-
$\alpha$ -tocotrienol	1.59	-
$\delta$ -tocopherol	2.40	28.32
$\gamma$ -tocopherol	30.47	42.63
$\alpha$ -tocopherol	15.65	1.50

## 2.2. Mixtures Preparation

Mixtures of PLA with (i) RBO and (ii) SO with concentrations of 1, 2 and 5 wt.% were prepared by using a MiniLab II HAAKE Rheomex CTW 5 (Waltham, MA, USA), a co-rotating conical twin-screw extruder, which allows mixing of the components. The mixing was performed at 180 °C, with a screw speed of 100 rpm and a recirculating time of 1.5 min. Before processing, PLA had been dried at a temperature of 60 °C for at least 24 h. The molten materials were transferred from the mini extruder through a preheated cylinder to a mini injection molder (Thermo Scientific HAAKE MiniJet II) (Waltham, MA, USA), which allows preparing dog-bone tensile bars specimens, to be used for thermal, mechanical, viscoelastic and morphological characterization. The mold temperature was 90 °C and the molding time 1 min. The dimensions of the dog-bone tensile bars were: Width in the larger section: 10 mm, width in the narrow section: 4.8 mm, thickness 1.35 mm, length 90 mm. For comparison, pure PLA was processed under the same conditions. After preparation, all the samples were stored in a desiccator to avoid moisture absorption, and analyzed the day after, to reduce physical ageing effects [36,37].

## 2.3. Mixtures Characterization

The thermal stability of RBO, SO and the PLA mixtures with RBO and SO was investigated by the thermogravimetric analysis (TGA) carried out on about 10 mg of sample by using a Perkin Elmer TGA

7 (Waltham, MA, USA), under nitrogen flow (35 mL/min), at a heating speed of 10 K/min from 50 °C to 600 °C.

Differential scanning calorimetry (DSC) measurements were performed with a Perkin Elmer Calorimeter DSC 8500 (Waltham, MA, USA), equipped with an IntraCooler III as refrigerating system. The instrument was calibrated in temperature with high purity standards (indium, naphthalene, cyclohexane) according to the procedure for standard DSC [38]. Energy calibration was performed with indium. Dry nitrogen was used as purge gas at a rate of 30 mL min<sup>-1</sup>. The as prepared PLA samples were analyzed from -50 °C to 200 °C at the heating rate of 10 K/min, after fast cooling from room temperature. Additional experiments were performed: The as prepared PLA, PLA + RBO (5 wt.%) and PLA + SO (5 wt.%) samples were melted at 180 °C for 0.5 min and successively fast cooled to 60 °C. After 5 min at 60 °C, the samples were heated at 100 K/min to 80 °C, and crystallized at this temperature for 60 min. The final heating scans were performed from -50 °C to 200 °C at the heating rate of 10 K/min, after fast cooling from 80 °C.

Tensile tests on the PLA mixtures prepared with the injection molder were performed at room temperature, at a crosshead speed of 10 mm/min, by means of an INSTRON 5500 R universal testing machine (Canton MA, USA), equipped with a 10kN load cell and interfaced with a computer running the Testworks 4.0 software (MTS Systems Corporation, Eden Prairie MN, USA). At least five specimens were tested for each sample in according to the ASTM D 638, and the average values reported.

Oscillatory shear measurements were performed by means of a Rheometer Anton Paar MCR 302 (Graz, Austria), equipped with parallel plates of 25 mm diameter, under nitrogen flow to minimize oxidation and to maintain dry environment. Frequency sweep experiments were performed at 175 °C at a fixed strain (3%), with a gap of 1 mm, in the linear regime, in order to measure the modulus of the complex viscosity  $|\eta^*|$  and the storage and loss moduli,  $G'$  and  $G''$ , respectively. The angular frequencies were swept from 0.01 to 628 Hz, with five points per decade.

The morphology of PLA mixtures was investigated by the scanning electron microscopy (SEM) with an FEG-Quanta 450 ESEM instrument (Waltham, MA, USA). The micrographs of samples fractured with liquid nitrogen and etched with gold were collected. Backscattered electrons generated the images with a resolution provided by the beam deceleration with a landing energy of 2 kV.

### 3. Results and Discussion

The thermal, morphological, mechanical, and viscoelastic properties of the PLA mixtures with RBO and SO were investigated in order to obtain information on possible miscibility/compatibility between the PLA and these natural oils, and to quantify how the addition of RBO and SO modifies the structure of the polymeric material.

#### 3.1. Thermogravimetric Analysis of RBO, SO, PLA, and PLA + RBO (5 wt.%) and PLA + SO (5 wt.%) Mixtures

The thermal stability of PLA, RBO, SO and the mixtures PLA+RBO (5 wt.%) and PLA+SO (5 wt.%) was determined by means of the thermogravimetric analysis under nitrogen flow, because the contact of the material with air is reduced in the extruder and moulder. Figure 1 shows that the degradation of PLA occurs in a single step, in a narrow temperature range. The initial degradation temperature is located at about 300 °C, whereas the maximum degradation rate is centred at about 360 °C, in excellent agreement with previous studies [13,26,39]. At temperatures higher than 300 °C, the thermal stability of SO appears slightly better than that of RBO and SO, in agreement with literature data [40]. For both oils, the initial main degradation temperature is close to 320 °C, whereas the maximum degradation rate is around 410 °C.

The addition of RBO and SO slightly improves the thermal stability of PLA, as reported also for other mixtures [13,41,42]. This behavior was explained by considering that the dispersion of the oils in the polymer matrix can act as a physical protective additive, which hinders and slows down the release of volatile degradation products, thus delaying the entire degradation process.

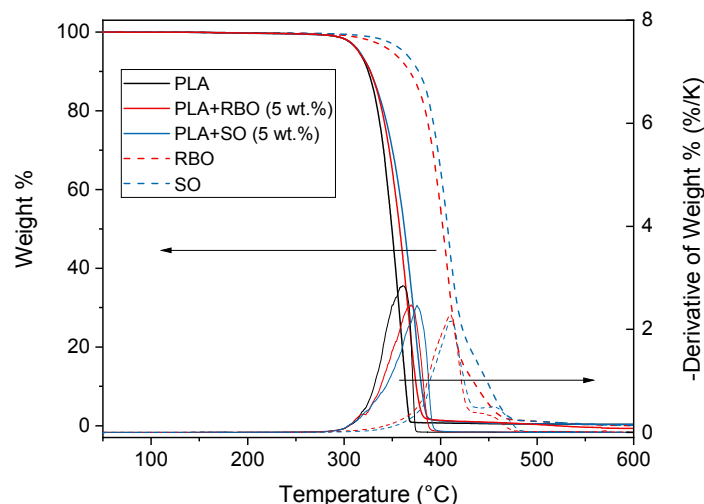


**Figure 1.** Thermogravimetric curves of poly(lactic acid) (PLA), RBO, SO and the mixtures PLA+RBO (5 wt.%) and PLA+SO (5 wt.%) at 10 K/min under nitrogen flow. The weight % curves are also shown (thin solid and dashed lines).

### 3.2. Morphological Properties of PLA and PLA + RBO (5 wt.%) and PLA + SO (5 wt.%) Mixtures

The morphology of fracture surfaces of PLA and PLA + RBO (5 wt.%) and PLA + SO (5 wt.%) from dog-bone specimens was studied by the scanning electron microscopy, in order to investigate the dispersion of the oils in the polymeric matrix.

Figure 2 illustrates the topology of the pure PLA, which appears smooth and without evident voids. This is the typical surface appearance of a fractured brittle material [43]. Conversely, many empty microvoids are observed in the fracture surfaces of the mixtures PLA+RBO (5 wt.%) and PLA + SO (5 wt.%). The presence of these numerous voids can be connected to phase separation between the PLA and excess oil, which is removed after the fracture with liquid nitrogen. A similar morphology has been reported for several PLA+oils or epoxidized oils mixtures [12,17,44,45].

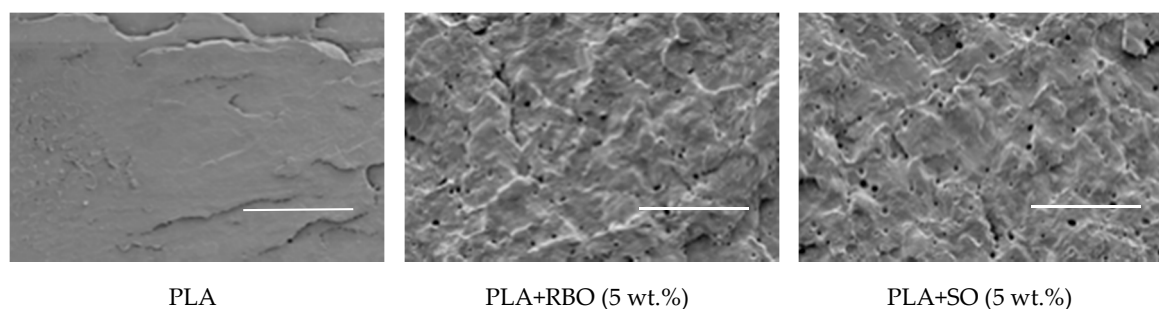


**Figure 2.** SEM images of the PLA and the PLA+RBO (5 wt.%) and PLA+SO (5 wt.%) mixtures. (The scale bar shows 30  $\mu\text{m}$ ).

### 3.3. Thermal Properties of PLA and PLA + RBO and PLA + SO Mixtures

The specific heat capacity ( $c_p$ ) curves of PLA and PLA mixed with RBO and SO with concentrations of 1, 2 and 5 wt.%, after molding at 90 °C for 1 min, are shown in Figures 3 and 4, respectively.

The glass transition temperature ( $T_g$ ), which is located in the proximity of 60 °C, in agreement with literature data [46], is overlapped by an enthalpy recovery peak, due to permanence of the samples at room temperatures for one day [36,37]. The  $T_g$  values do not appear to decrease in the presence of RBO and SO. This could mean that both RBO and SO do not act as efficient plasticizers for PLA at a concentration lower than 5 wt.%. Before the melting endotherm, all the curves display an intense cold-crystallization peak located approximately in the interval between 85 °C and 130 °C.

At temperatures lower than about 100 °C, the crystal  $\alpha'$ -form of PLA mainly grows, whereas in the temperature range from 100 °C and 120 °C, a mixture of  $\alpha'$ - and  $\alpha$ -forms develops [47]. The two crystal modifications have a similar chain packing, but the lattice dimensions of  $\alpha'$ -crystals are slightly larger than the  $\alpha$  counterpart. The  $\alpha'$ -phase is indeed characterized by loose chain-packing and conformational disorder, which leads to different physical and mechanical properties in comparison with the  $\alpha$ -phase [48].

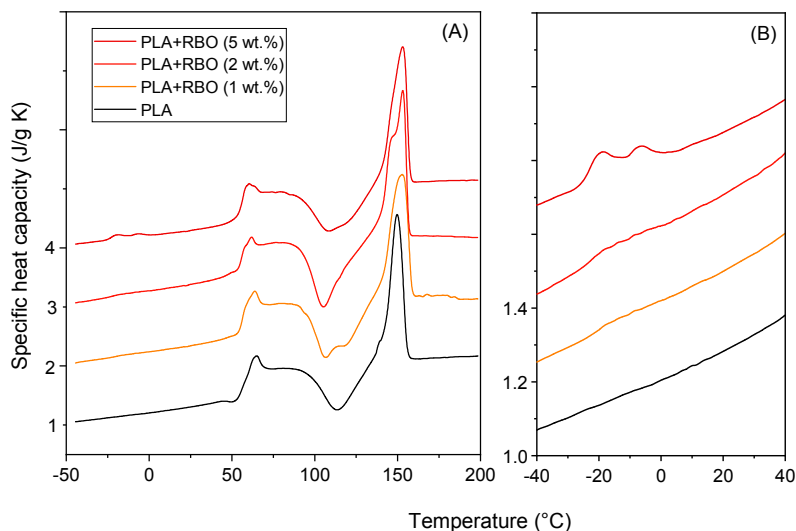


**Figure 3.** (A) Specific heat capacity ( $c_p$ ) of PLA and the PLA mixed with RBO at the concentrations indicated, as a function of the temperature. The curves were measured upon heating at 10 K/min after previous fast cooling to  $-50$  °C; (B) enlargement of the  $c_p$  curves in the sub  $T_g$  region. The ordinate values refer only to the bottom curves. All the other curves are shifted vertically for the sake of clearness.

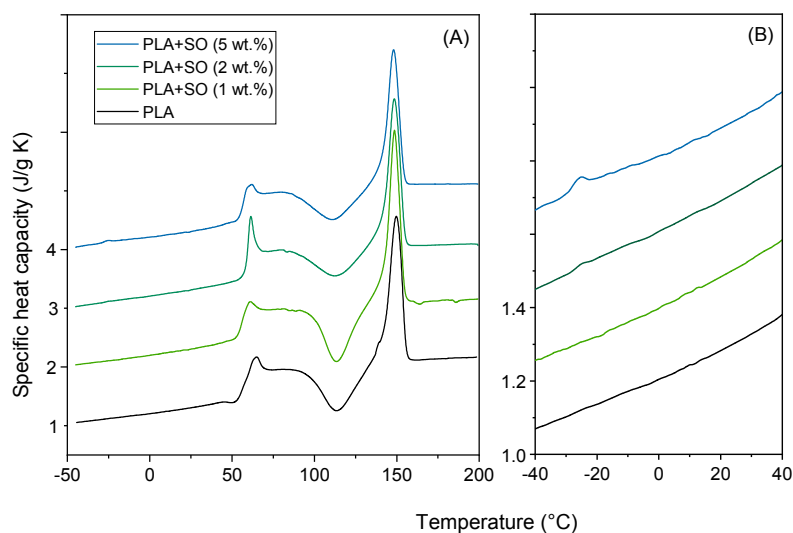


**Figure 4.** (A) Specific heat capacity ( $c_p$ ) of PLA and the PLA mixed with SO at the concentrations indicated, as a function of the temperature. The curves were measured upon heating at 10 K/min after previous fast cooling to  $-50$  °C; (B) enlargement of the  $c_p$  curves in the sub  $T_g$  region. The ordinate values refer only to the bottom curves. All the other curves are shifted vertically for the sake of clearness.

At the heating rate of 10 °C/min, the  $\alpha'$ -crystals transform into the more ordered  $\alpha$ -phase by melting and almost simultaneous recrystallization, which cannot be distinguished separately [49]. As a consequence, the melting behavior that extends from approximately 130 °C to 165 °C (see Figures 3A and 4A), results from the fusion of both the  $\alpha'$ - and the  $\alpha$ -crystals. Reorganization and recrystallization

events overlap the entire fusion process, as generally takes place in semi-crystalline polymers at a relatively low heating rate [50,51].

The enlargements of the  $c_p$  curves in the sub  $T_g$  regions, depicted in Figures 3B and 4B, display an endothermic event between  $-30$  and  $5$  °C, which has to be connected with the fusion of the oils. The endothermic process is more pronounced with increasing the oil content, and is appreciable for  $\text{RBO} \geq 1$  wt.% and  $\text{SO} \geq 2$  wt.%. In effects  $c_p$  curves of pure RBO and SO, obtained after fast cooling down to  $-50$  °C, exhibit multiple endothermic processes in the temperature range between  $-50$  °C and  $10$  °C (Figure 5). These peaks are ascribable to the complex fusion of the triacylglycerols (TAGs), the main components of the oils, which are present in different concentrations in RBO and SO, as deduced from Table 1. The shape of the peaks is multiple, due to the many crystalline forms (polymorphism) present in the solid TAGs mixtures [52]. The TAG crystals grown upon fast cooling down to  $-50$  °C reorganize and recrystallize upon heating at  $10$  K/min, transforming from one crystalline phase into a different one [53–55]. The measured enthalpies of fusion ( $\Delta h_{m,oil}^\circ$ ) of pure RBO and SO are  $61$  J/g and  $58$  J/g, respectively. The RBO and SO separate phases observed in Figures 3 and 4 at low temperatures attest that PLA and the oils are not completely miscible. RBO and SO partially crystallize as separate phases upon cooling, and this proves that specific and strong interactions between PLA and (i) RBO and (ii) SO are not established in the mixtures.

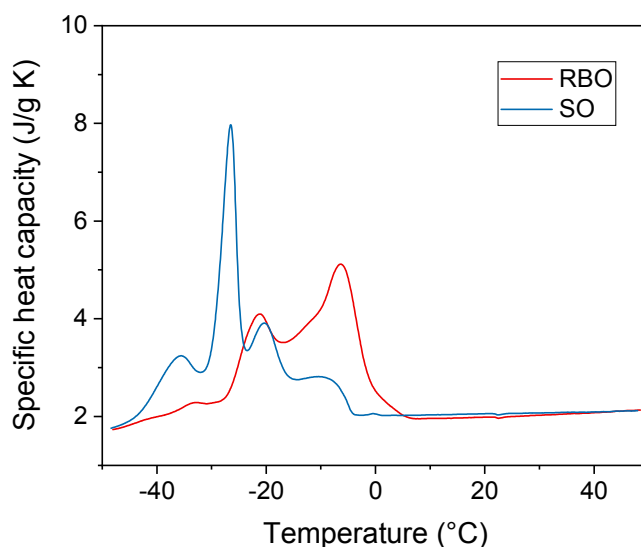


**Figure 5.** Specific heat capacity ( $c_p$ ) of pure RBO and SO and upon heating at  $10$  K/min after previous fast cooling to  $-50$  °C.

An estimation of the amount of the separate oil in the mixtures was performed by comparing the enthalpy of fusion ( $\Delta h_m$ ) of the oils in the PLA+RBO and PLA+SO mixtures (calculated from Figures 3 and 4), with the enthalpy of fusion of pure RBO and SO (determined from Figure 5). Table 3 shows the  $\Delta h_m$  values, derived from Figures 3 and 4, and the corresponding  $\Delta h_{m,oil}$  values, obtained after normalization to the oil concentration. The comparison between  $\Delta h_{m,oil}$  and the enthalpy of fusion of 100% pure oils ( $\Delta h_{m,oil}^\circ$ ) suggests that not all the oil added to the PLA separates, so that a partial miscibility/compatibility exists between the PLA and (i) RBO and (ii) SO. With respect to RBO, SO appears more miscible with PLA. By considering the oil amount that separates, an estimation of the effective oil mixed with PLA was thus achieved, as listed in Table 3 (last column). The data collected in Table 3 reveal that the percentage of oil mixed with PLA increases with the nominal oil amount, which suggests that a longer mixing time could favor the incorporation of the oil to PLA. The present cycle time of  $1.5$  min was however chosen because it was similar to the operating conditions generally used for productive processes.

**Table 3.** Enthalpy of fusion of the RBO and SO separate phases in the mixtures PLA + RBO and PLA + SO ( $\Delta h_m$  and  $\Delta h_{m,oil}$ ) and effective oil mixed with PLA (wt.%).

Formulation	$\Delta h_m$ (J/g <sub>mixture</sub> )	$\Delta h_{m,oil}$ (J/g <sub>oil</sub> )	Effective Mixed Oil (wt.%)
PLA + RBO (1 wt.%)	0.20	20.0	0.67
PLA + RBO (2 wt.%)	0.45	22.5	1.25
PLA + RBO (5 wt.%)	1.24	24.8	2.93
PLA + SO (1 wt.%)	-	-	1.00
PLA + SO (2 wt.%)	0.15	7.5	1.74
PLA + SO (5 wt.%)	0.36	7.2	4.38

Table 4 lists the PLA enthalpy of cold crystallization ( $\Delta h_c$ ) and the enthalpy of fusion ( $\Delta h_m$ ) calculated from the  $c_p$  curves shown in Figures 3 and 4 after the construction of a linear baseline from approximately 80 °C to 165 °C. The  $\Delta h_c$  and  $\Delta h_m$  values collected in Table 4 are normalized to the PLA content. From these experimental values, an estimation of the crystalline weight fraction growing during the cold crystallization process ( $w_{Cc}$ ), and disappearing during the melting process ( $w_{Cm}$ ) was thus obtained, dividing  $\Delta h_c$  and  $\Delta h_m$  by the enthalpy of fusion of 100% crystalline PLA phase ( $\Delta h_m^\circ$ ) at the crystallization and melting peak temperatures, respectively. As both  $\alpha'$ - and  $\alpha$ -forms grow during cold crystallization, and disappear during the melting process, average values between the enthalpy of fusion of the  $\alpha'$ - and  $\alpha$ -forms were utilized [56], i.e.,  $\Delta h_m^\circ = 99$  J/g for the cold crystallization centered at about 105 °C,  $\Delta h_m^\circ = 101$  J/g for the cold crystallization centered at about 110 °C,  $\Delta h_m^\circ = 103$  J/g for the cold crystallization centered at about 114 °C, and  $\Delta h_m^\circ = 119$  J/g for the melting process centered approximately at 150 °C. The crystalline weight fraction of the as prepared samples ( $w_c$ ) was determined as the difference ( $w_{Cm} - w_{Cc}$ ). The  $w_c$  values listed in Table 4 reveal that the crystallinity degree of the as prepared PLA samples is very low. This can be explained by considering the small times that characterize a typical injection molding and the slow crystallization kinetics of PLA [57]. A slightly higher crystallinity is exhibited by the PLA + SO mixtures, which are characterized by higher effective oil content. This suggests that at the moulding temperature of 90 °C, the mobility of the PLA chains is higher in the PLA + SO mixtures, due to the higher miscibility of SO with PLA.

**Table 4.** Enthalpy of cold crystallization ( $\Delta h_c$ ), enthalpy of fusion ( $\Delta h_m$ ), and crystalline weight fraction growing during cold crystallization ( $w_{Cc}$ ) and disappearing during fusion ( $w_{Cm}$ ) for the PLA + RBO and PLA + SO mixtures, after molding at 90 °C for 1 min (estimated errors:  $\pm 1$  J/g for  $\Delta h_c$  and  $\Delta h_m$ ;  $\pm 0.02$  for  $w_{Cc}$  and  $w_{Cm}$ , and  $\pm 0.04$  for  $w_c$ ).

	$\Delta h_c$ (J/g)	$w_{Cc}$	$\Delta h_m$ (J/g)	$w_{Cm}$	$w_c$
PLA	14.4	0.14	24.3	0.20	0.06
PLA + RBO (1 wt.%)	21.6	0.21	26.8	0.23	0.02
PLA + RBO (2 wt.%)	21.7	0.21	28.7	0.24	0.03
PLA + RBO (5 wt.%)	18.8	0.19	27.3	0.23	0.04
PLA + SO (1 wt.%)	15.7	0.15	26.0	0.22	0.07
PLA + SO (2 wt.%)	11.8	0.12	22.7	0.19	0.07
PLA + SO (5 wt.%)	12.0	0.12	22.6	0.19	0.07

More remarkable is the position and the shape of the cold-crystallization peaks (Figures 3 and 4). The cold-crystallization peaks of the mixtures are located at slightly lower temperatures with respect to the pure PLA. This means that the mixtures are characterized by a higher chain mobility, which induces crystallization at lower temperatures. The cold-crystallization process of the pure PLA appears as a single peak, as well as that of the PLA + SO mixtures. Conversely, the PLA + RBO mixtures exhibit an asymmetric exothermic peak, which is double and well resolved for the PLA + RBO (1 wt.%)



mixture. It is well known from the literature that in the temperature range 100–120 °C both the  $\alpha'$ - and  $\alpha$ -forms grow in PLA [47]. The peak observed at lower temperatures is ascribable to the growth of  $\alpha'$ -crystals, whereas the peak at higher temperatures to the development of the  $\alpha$ -phase. Thus, Figure 3 suggests that the crystallization of the  $\alpha'$ -phase is favored in the PLA + RBO mixtures.

In the attempt to confirm this hypothesis, additional experiments were performed, as described in the Materials and Method section. The as prepared PLA, PLA + RBO (5 wt.%) and PLA + SO (5 wt.%) samples, after fusion, were annealed at 60 °C for 5 min, to allow the formation of crystal nuclei which accelerate subsequent crystallization at temperatures above  $T_g$  [58]. The  $c_p$  curves of the samples crystallized at 80 °C for 1 h, after nucleation for 5 min at 60 °C, are displayed in Figure 6. For the PLA + RBO (5 wt.%) sample, the crystallization time of 1 h is sufficient to complete crystallization at 80 °C, because the relative  $c_p$  curve shows that cold crystallization during the successive heating run is absent. Conversely, crystallization at 80 °C is not complete for the PLA + SO (5 wt.%) sample, which undergoes cold crystallization between 80 and 120 °C. Cold crystallization is much more intense for pure PLA, which means that the addition of the oils improves the mobility of the chains and favors PLA crystallization. The enthalpies of fusion, calculated as  $\Delta h = \Delta h_m - \Delta h_c$  and normalized to the PLA content, are indeed 18, 29 and 35 J/g for PLA, PLA + SO (5 wt.%) and PLA + RBO (5 wt.%), respectively. That  $\alpha'$ -form grows at 80 °C is attested by the exotherm at about 135 °C, which is connected with the reorganization of the  $\alpha'$ -crystals into  $\alpha$ -crystals [59]. This exotherm is barely visible in the  $c_p$  curve of pure PLA, which further confirms the slower and reduced formation of  $\alpha'$ -crystals at 80 °C in the absence of the oils. These experiments prove that both RBO and SO favor the growth of PLA  $\alpha'$ -crystals, and that RBO is more efficient than SO, being the relative  $\Delta h$  value higher and the effective concentration lower. The promoting of the  $\alpha'$ -crystallization could be ascribed to a nucleant effect exerted by the separate liquid oil microdroplets. The different composition of the unsaponifiable matter of RBO and SO, i.e., tocotrienols, tocopherols and especially  $\gamma$ -oryzanol, which is present in high percentage in RBO, could be the cause of the different nucleating action for the PLA  $\alpha'$ -form. Future investigations on the PLA crystalline growth in the presence of additional increasing amount of  $\gamma$ -oryzanol could better clarify this issue.

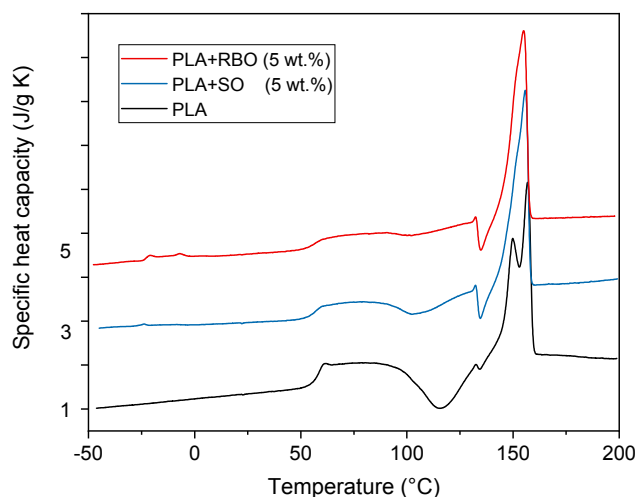


**Figure 6.** Specific heat capacity ( $c_p$ ) of pure PLA and PLA + RBO (5 wt.%) and PLA + SO (5 wt.%) as a function of the temperature. The curves were measured upon heating at 10 K/min after nucleation at 60 °C for 5 min, crystallization at 80 °C for 1h, and fast cooling to −50 °C.

#### 3.4. Mechanical Properties of PLA and PLA + RBO and PLA + SO Mixtures

The mechanical properties of pure PLA and the PLA + RBO and PLA + SO mixtures are summarized in Figure 7, which displays that the elastic modulus does not change as a result of the addition of RBO and SO up to a content of 5 wt.%, whereas the tensile strength decreases markedly and the elongation at break strongly increases.

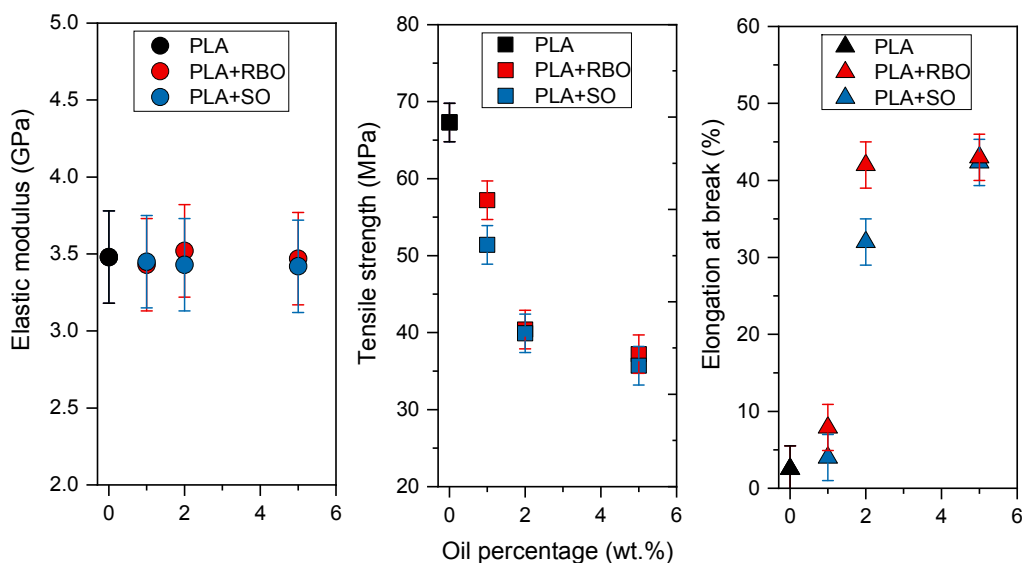


**Figure 7.** Elastic modulus, tensile strength and elongation at break of PLA and the PLA + RBO and PLA + SO mixtures as a function of the oil percentage.

As a general rule, the addition of a plasticizer leads to a progressive decrease in the elastic modulus and tensile strength, whereas an increase in elongation at break is usually detected, due to the increased polymer flexibility. [8,60,61]. Similar trends have been observed for PLA plasticized with epoxidized oils, for which a good plasticizing effect on PLA was proved [13,14,17,19,41,42].

Both the drop in tensile strength and the increase in the elongation at break can be connected to the action exerted by the oil, either mixed or separate. Not only the oil effectively mixed, but also the oil microdroplets, dispersed within the polymeric matrix, can act as a lubricant, by reducing the forces of attraction between the polymer molecules and by increasing the flexibility of the chains. The plastic deformation of PLA comes out promoted, and brittleness reduced. The unchanged elastic modulus can be rationalized by considering that it is calculated in the initial linear stress vs. strain region. For very small deformations, the effect of a low percentage of added oil can be negligible, especially if the miscibility is scarce.

### 3.5. Viscoelastic Properties of PLA and PLA + RBO and PLA + SO Mixtures

The study of the viscoelastic properties is crucial to gain a fundamental understanding of the processability of a polymeric material. In addition, for a mixture, it provides information on the state of dispersion of the components. The flow behavior of a polymer melt is generally defined by the viscosity, i.e., the ratio of the stress to the deformation rate. For common liquids, the viscosity is dependent only on the temperature and pressure, and not on the deformation rate and time. The situation is much more complicated for polymeric liquids, because viscosity depends also on the deformation conditions. Polymer melts are in fact viscoelastic materials, because flow is accompanied also by elastic effects. The melt viscosity of polymers is very sensitive to changes in the macromolecular chain structure and the addition of plasticizers, which increase the polymer free volume and the polymer chain mobility. Viscoelastic properties are generally measured through dynamic shear experiments, because from oscillatory measurements details on both the elastic and viscous properties can be obtained [62]. Dynamic oscillatory shear measurements of polymeric materials are generally performed by applying a time dependent strain  $\gamma(t) = \gamma_0 \cdot \sin(\omega t)$ , and measuring the resultant shear stress  $\sigma(t) = \sigma_0 \cdot [G' \sin(\omega t) + G'' \cos(\omega t)]$ , where  $G'$  and  $G''$  are the storage and loss moduli, respectively and  $\omega$  is the angular frequency. In addition, the modulus of the complex viscosity  $|\eta^*|$  can be derived, as it holds that  $|\eta^*(\omega)| = [G'(\omega)^2 + G''(\omega)^2]^{1/2} / \omega$  [62].

The bilogarithmic plot of  $|\eta^*|$  vs.  $\omega$  obtained by the parallel plate oscillating rheometer at 175 °C for PLA and the PLA/RBO (5 wt.%) and PLA/SO (5 wt.%) mixtures is shown in Figure 8. The experiments were performed from low to high frequencies. All the curves indicate a decrease in the complex viscosity with increasing the deformation frequency. In general, PLA behaves like a pseudo-plastic, non-Newtonian fluid, and a typical shear thinning fluid, in which at high shear rates the macromolecules orient and the entanglements number decreases [63,64]. Actually also in the terminal zone at low frequency, which defines the zero-shear viscosity  $\eta_0$ , a small decrease in viscosity is observed for pure PLA, probably due to an original strongly entangled structure not completely destroyed before the beginning of the rheological test. The  $\eta_0$  value for PLA at 175 °C is about  $5.8 \cdot 10^6$  mPa s. This value is in the range typical of commercial PLA ( $M_w = 140$ – $160$  kg/mol), i.e.,  $10^5$ – $10^7$  mPa s [65].

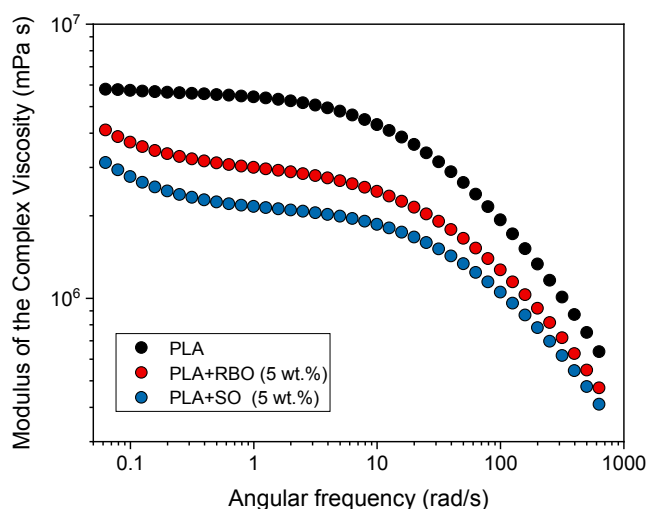


**Figure 8.** Modulus of the complex viscosity ( $|\eta^*|$ ) as a function of the angular frequency ( $\omega$ ) at 175 °C for PLA and the PLA+RBO (5 wt.%) and PLA+SO (5 wt.%) mixtures.

The incorporation of RBO and SO reduces the viscosity, suggesting that both RBO and SO influence the relaxation times of PLA. The viscosity decreases at a higher extent in the presence of SO, due to the higher concentration of the oil actually mixed to PLA. Both the PLA/RBO (5 wt.%) and PLA/SO (5 wt.%) mixtures exhibit a strong shear thinning behavior also at low angular frequencies. This behavior has to be ascribed to the change in the shape of the oil droplets, which elongate in the direction of the flow, thus increasing the surface contact with the polymer chains and the free volume in the mixtures. The intermolecular forces between the polymer chains weaken, and the PLA mobility increases. In this way the oils act as lubricants, reducing friction and facilitating polymer chain mobility [7]. The final effect of the addition of RBO and SO to PLA is thus similar to that of a classical plasticizer [14,66].

The storage and loss moduli ( $G'$  and  $G''$ ) of PLA and the PLA+RBO (5 wt.%) and PLA + SO (5 wt.%) mixtures are shown in Figure 9. Both  $G'$  and  $G''$  of PLA present the typical liquid-like behavior of molten polymers, with the slope of the  $G'$  and  $G''$  curves in the terminal zone equal to 2 and 1, respectively. The viscous nature is dominant at low frequencies, when  $G'' > G'$ , whereas the elastic properties are dominant at high frequencies, when  $G' > G''$ . The slopes of  $G'$  and  $G''$  for the PLA + RBO (5 wt.%) and PLA + SO (5 wt.%) mixtures are slightly lower with respect to PLA, as well as the values of  $G'$  and  $G''$  at all the investigated frequencies. The lower  $G'$  values of the mixtures with respect to PLA can be ascribed to more mobile chains in the presence of both RBO and SO. On the other hand, the order of the  $G''$  curves appears similar to that of the viscosity (PLA > PLA + RBO > PLA + SO), because it represents the viscous part of the stress, i.e., the part of the stress where energy is dissipated.

The  $G'$ — $G''$  cross point shifts towards higher frequencies in the case of the mixtures, indicating that the relaxation times in the melt decreases in the presence of RBO and SO. The material starts to flow ( $G'' > G'$ ) when the stress applied is higher than intermolecular forces. The fact that this

occurs in the mixtures at higher deformation frequency means that the oils cause a weakening of the intermolecular interactions between the PLA chains, and an increase in the intermolecular spaces, which results in a decrease in the relaxation times.

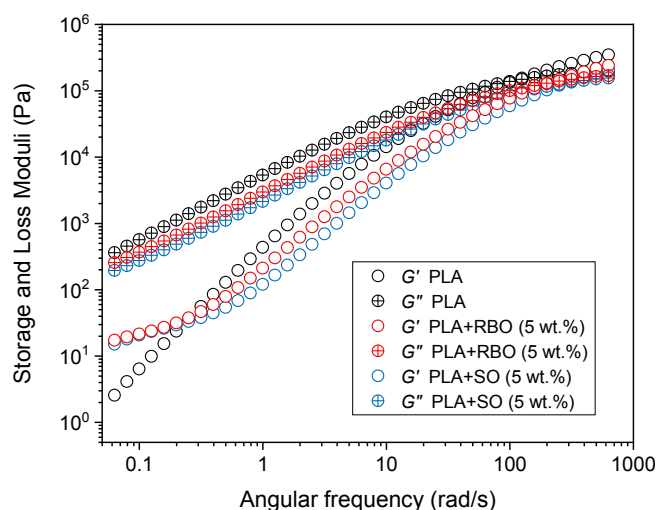


**Figure 9.** Storage modulus ( $G'$ ) and loss modulus ( $G''$ ) as a function of the angular frequency ( $\omega$ ) at 175 °C for PLA and the PLA + RBO (5 wt.%) and PLA + SO (5 wt.%) mixtures.

#### 4. Conclusions

In this study the utilization of natural oils, in particular RBO and SO, as possible plasticizers for PLA has been investigated. This is the first time that RBO is taken into consideration for this possible application.

Both RBO and SO are not completely miscible with PLA, as they are observed as separate phases at low temperature. However, certain compatibility exists between PLA and (i) RBO and (ii) SO, because the demixing is not complete.

Although not totally miscible/compatible, RBO and SO are able to reduce the viscosity of the PLA + RBO and PLA + SO mixtures, which proves that the addition of RBO and SO to PLA reduces the intermolecular forces, and increases the mobility of the PLA polymeric chains. This finding attests that a small amount of RBO or SO can be successfully added to PLA to improve its processability.

In addition, the mechanical properties of the PLA+RBO and PLA+SO mixtures (elastic modulus, tensile strength and elongation at break) are different with respect to the pure PLA, with trends typical of plasticizer-polymer systems. A comparison between these trends and literature data for PLA plasticized with epoxidized vegetable oils showed that the mechanical properties are on average comparable [15,19]. The epoxidized vegetable oils exhibit a higher miscibility/compatibility with PLA, but on the other hand they are more expensive and not totally eco-friendly, because they are prepared by chemical synthesis. This validates the utilization of RBO and SO as plasticizers for PLA, although they are not completely miscible with PLA.

More interestingly, RBO was found to accelerate the growth of the PLA  $\alpha'$ -crystals at low crystallization temperatures. This feature is appealing, because the  $\alpha'$ -phase presents lower elastic modulus and higher permeability to water vapor in comparison to the  $\alpha$ -phase, which grows at high temperatures [67,68]. This means that PLA materials processed at different temperatures can exhibit different properties. The present study has demonstrated that the addition of completely natural RBO to PLA in small percentages is a useful solution for a faster preparation of PLA materials containing mainly the  $\alpha'$ -phase, according to the principles of circular economy, in order to favor the production of sustainable polymeric materials with properties useful for practical applications.

**Author Contributions:** M.C.R. contributed to funding acquisition and conceptualization of the study, supervised the work, wrote and reviewed the paper; P.C. contributed to funding acquisition and reviewed the paper; N.M.

performed the mechanical, thermal and morphological characterization; C.A.M. performed the viscoelastic characterization; M.I. performed the oil chemical characterization and reviewed the paper; A.L. contributed to funding acquisition and reviewed the paper.

**Funding:** This research was funded by the European Commission's Horizon 2020 Research and Innovation Programme (2014–2020)—Sustainable techno-economic solutions for the agricultural value chain (AgroCycle), under Grant Agreement n. 690142.

**Conflicts of Interest:** The authors declare no conflict of interest.

## References

1. Reddy, M.M.; Vivekanandhan, S.; Misra, M.; Bhatia, S.K.; Mohanty, A.K. Biobased plastics and bionanocomposites: Current status and future opportunities. *Prog. Polym. Sci.* **2013**, *38*, 1653–1689. [[CrossRef](#)]
2. Tang, H.; Luan, Y.; Yang, L.; Sun, H. A Perspective on Reversibility in Controlled Polymerization Systems: Recent Progress and New Opportunities. *Molecules* **2018**, *23*, 2870. [[CrossRef](#)] [[PubMed](#)]
3. Perego, G.; Cella, G.D. Mechanical Properties. In *Poly(lactic acid): Synthesis, Properties, Processing, and Applications*; Auras, R., Lim, L.-T., Selke, S.E.M., Tsuji, H., Eds.; John Wiley & Sons: Hoboken, NJ, USA, 2010; pp. 141–153.
4. Farah, S.; Anderson, D.G.; Langer, R. Physical and mechanical properties of PLA, and their functions in widespread applications—A comprehensive review. *Adv. Drug. Deliver. Rev.* **2016**, *107*, 367–392. [[CrossRef](#)] [[PubMed](#)]
5. Gurgel Adeodato Vieira, M.; Altenhofen da Silva, M.; Oliveira dos Santos, L.; Masumi Beppu, M. Natural-based plasticizers and biopolymer films: A review. *Eur. Polym. J.* **2011**, *47*, 254–263. [[CrossRef](#)]
6. Wypych, G. (Ed.) *Handbook of Plasticizers*, 3rd ed.; ChemTec Publishing: Toronto, ON, Canada, 2017.
7. Mekonnen, T.; Mussone, P.; Khalil, H.; Bressler, D. Progress in bio-based plastics and plasticizing modifications. *J. Mater. Chem. A* **2013**, *1*, 13379–13398. [[CrossRef](#)]
8. Labrecque, L.V.; Kumar, R.A.; Davè, V.; Gross, R.A.; Mccarthy, S.P. Citrate esters as plasticizers for poly(lactic acid). *J. Appl. Polym. Sci.* **1997**, *66*, 1507–1513. [[CrossRef](#)]
9. Martin, O.; Averous, L. Poly(lactic acid): Plasticization and properties of biodegradable multiphase systems. *Polymer* **2001**, *42*, 6209–6219. [[CrossRef](#)]
10. Darie-Nita, R.N.; Vasile, C.; Irimia, A.; Lipsa, R.; Rapa, M. Evaluation of some eco-friendly plasticizers for PLA films processing. *J. Appl. Polym. Sci.* **2016**, *133*, 43223–43234. [[CrossRef](#)]
11. Burgos, N.; Martino, V.P.; Jimenez, A. Characterization and ageing study of poly(lactic acid) films plasticized with oligomeric lactic acid. *Polym. Derad. Stab.* **2013**, *98*, 651–658. [[CrossRef](#)]
12. Ferri, J.M.; Samper, M.D.; Garcia-Sanoguera, D.; Reig, M.J.; Fenollar, M.J.; Balart, R. Plasticizing effect of biobased epoxidized fatty acid esters on mechanical and thermal properties of poly(lactic acid). *J. Mater. Sci.* **2016**, *51*, 5356–5366. [[CrossRef](#)]
13. Jaffar Al-Mulla, E.A.; Zin Wan Yunus, W.M.; Bt Ibrahim, N.A.; Rahman, M.Z.A. Properties of epoxidized palm oil plasticized polylactic acid. *J. Mater. Sci.* **2010**, *45*, 1942–1946. [[CrossRef](#)]
14. Xu, Y.-Q.; Qu, J.-P. Mechanical and Rheological Properties of Epoxidized Soybean Oil Plasticized Poly(lactic acid). *J. Appl. Polym. Sci.* **2009**, *112*, 3185–3191. [[CrossRef](#)]
15. Carbonell-Verdu, A.; Garcia-Garcia, D.; Dominici, F.; Torre, L.; Sanchez-Nacher, L.; Balart, R. PLA films with improved flexibility properties by using maleinized cottonseed oil. *Eur. Polym. J.* **2017**, *91*, 248–259. [[CrossRef](#)]
16. Ferri, J.M.; Garcia-Garcia, D.; Montanes, N.; Fenollar, O.; Balart, R. The effect of maleinized linseed oil as biobased plasticizer in poly(lactic acid)-based formulations. *Polym. Int.* **2017**, *66*, 882–891. [[CrossRef](#)]
17. Carbonell-Verdu, A.; Samper, M.D.; Garcia-Garcia, D.; Sanchez-Nacher, L.; Balart, R. Plasticization effect of epoxidized cottonseed oil (ECSO) on poly(lactic acid). *Ind. Crop. Prod.* **2017**, *104*, 278–286. [[CrossRef](#)]
18. Xing, C.; Matuana, L.M. Epoxidized soybean oil-plasticized poly(lactic acid) films performance as impacted by storage. *J. Appl. Polym. Sci.* **2016**, *133*, 43201–43209. [[CrossRef](#)]
19. Chieng, B.W.; Ibrahim, N.A.; Then, Y.Y.; Loo, Y.Y. Epoxidized Vegetable Oils Plasticized Poly(lactic acid) Biocomposites: Mechanical, Thermal and Morphology Properties. *Molecules* **2014**, *19*, 16024–16038. [[CrossRef](#)] [[PubMed](#)]

20. Orue, A.; Eceiza, A.; Arbelaiz, A. The effect of sisal fiber surface treatments, plasticizer addition and annealing process on the crystallization and the thermo-mechanical properties of poly(lactic acid) composites. *Ind. Crop. Prod.* **2018**, *118*, 321–333. [[CrossRef](#)]
21. Orue, A.; Eceiza, A.; Arbelaiz, A. Preparation and characterization of poly(lactic acid) plasticized with vegetable oils and reinforced with sisal fibers. *Ind. Crops Prod.* **2018**, *112*, 170–180. [[CrossRef](#)]
22. Balart, J.F.; Fombuena, V.; Fenollar, O.; Boronat, T.; Sanchez-Nacher, L. Processing and characterization of high environmental efficiency composites based on PLA and hazelnut shell flour (HSF) with biobased plasticizers derived from epoxidized linseed oil (ELO). *Compos. Part B* **2016**, *86*, 168–177. [[CrossRef](#)]
23. Xia, Y.; Larock, R.C. Vegetable Oil-Based Polymeric Materials: Synthesis, Properties, and Applications. *Green Chem.* **2010**, *12*, 1893–1909. [[CrossRef](#)]
24. Belgacem, M.N.; Gandini, A. Materials from Vegetable Oils: Major Sources, Properties and Applications. In *Monomers, Polymers and Composites from Renewable Resources*, 1st ed.; Elsevier: Oxford, UK, 2008; pp. 39–66.
25. Jia, P.; Xia, H.; Tang, K.; Zhou, Y. Plasticizers derived from Biomass Resources: A short Review. *Polymers* **2018**, *10*, 1303. [[CrossRef](#)] [[PubMed](#)]
26. Mele, G.; Bloise, E.; Cosentino, F.; Lomonaco, D.; Avelino, F.; Marciànò, T.; Massaro, C.; Mazzetto, S.E.; Tammaro, L.; Scalone, A.G.; et al. Influence of Cardanol Oil on the Properties of Poly(lactic acid) Films, Produced by Melt Extrusion. *ACS Omega* **2019**, *4*, 718–726. [[CrossRef](#)]
27. Bhasney, S.M.; Patwa, R.; Kumar, A.; Katiyar, V. Plasticizing effect of coconut oil on morphological, mechanical, thermal, rheological, barrier, and optical properties of poly(lactic acid): A promising candidate for food packaging. *J. Appl. Polym. Sci.* **2017**, *134*, 45390–45402. [[CrossRef](#)]
28. Friedman, J. Rice brans, rice bran oils, and rice hulls: Composition, food and industrial uses, and bioactivities in humans, animals, and cells. *J. Agric. Food Chem.* **2013**, *61*, 10626–10641. [[CrossRef](#)] [[PubMed](#)]
29. Sohail, M.; Rakha, A.; Butt, M.S.; Iqbal, M.J.; Rashid, S. Rice bran nutraceuticals: A comprehensive review. *Crit. Rev. Food Sci. Nutr.* **2017**, *57*, 3771–3780. [[CrossRef](#)] [[PubMed](#)]
30. Mohanty, A.K.; Vivekanandhan, S.; Pin, J.-M.; Misra, M. Composites from renewable and sustainable resources: Challenges and innovations. *Science* **2018**, *362*, 536–542. [[CrossRef](#)]
31. Väisänen, T.; Haapala, A.; Lappalainen, R.; Tomppo, L. Utilization of agricultural and forest industry waste and residues in natural-polymer composites. A review. *Waste Manag.* **2016**, *54*, 62–73. [[CrossRef](#)] [[PubMed](#)]
32. Righetti, M.C.; Cinelli, P.; Mallegni, N.; Stabler, A.; Lazzeri, A. Thermal and Mechanical Properties of Biocomposites Made of Poly(3-hydroxybutyrate-co-3-hydroxyvalerate) and Potato Pulp Powder. *Polymers* **2019**, *11*, 308. [[CrossRef](#)] [[PubMed](#)]
33. Righetti, M.C.; Cinelli, P.; Mallegni, N.; Massa, C.A.; Bronco, S.; Stabler, A.; Lazzeri, A. Thermal, Mechanical, and Rheological Properties of Biocomposites Made of Poly(lactic acid) and Potato Pulp Powder. *Int. J. Mol. Sci.* **2019**, *20*, 675. [[CrossRef](#)]
34. Righetti, M.C.; Cinelli, P.; Mallegni, N.; Massa, C.A.; Aliotta, L.; Lazzeri, A. Thermal, Mechanical, Viscoelastic and Morphological Properties of Poly(lactic acid) based Biocomposites with Potato Pulp Powder Treated with Waxes. *Materials* **2019**, *12*, 990. [[CrossRef](#)] [[PubMed](#)]
35. Irakli, M.; Kleisiaris, F.; Mygdalia, A.; Katsantonis, D. Stabilization of rice bran and its effect on bioactive compounds content, antioxidant activity and storage stability during infrared radiation heating. *J. Cereal Sci.* **2018**, *80*, 135–142. [[CrossRef](#)]
36. Righetti, M.C.; Gazzano, M.; Delpouve, N.; Saiter, A. Contribution of the rigid amorphous fraction to physical ageing of semi-crystalline PLLA. *Polymer* **2017**, *125*, 241–253. [[CrossRef](#)]
37. Hutchinson, J.M. Physical ageing of polymers. *Prog. Polym. Sci.* **1995**, *20*, 703–760. [[CrossRef](#)]
38. Sarge, S.M.; Hemminger, W.; Gmelin, E.; Höhne, G.W.H.; Cammenga, H.K.; Eysel, W. Metrologically based procedures for the temperature, heat and heat flow rate calibration of DSC. *J. Therm. Anal.* **1997**, *49*, 1125–1134. [[CrossRef](#)]
39. McNeill, I.C.; Leiper, H.A. Degradation Studies of Some Polyesters and Polycarbonates.—1. Polylactide: General Features of the Degradation Under Programmed Heating Conditions. *Poly. Degrad. Stab.* **1985**, *1*, 264–285. [[CrossRef](#)]
40. Santos, J.C.O.; Dos Santos, I.M.G.; De Souza, A.G.; Prasad, S.; Dos Santos, A.V. Thermal stability and kinetic study on thermal decomposition of commercial edible oils by thermogravimetry. *J. Food Sci.* **2002**, *67*, 1393–1398. [[CrossRef](#)]

41. Chieng, B.W.; Ibrahim, N.A.; Then, Y.Y.; Loo, Y.Y. Epoxidized Jatropha Oil as a Sustainable Plasticizer to Poly(lactic Acid). *Polymers* **2017**, *9*, 204. [[CrossRef](#)]
42. Silverajah, V.S.; Ibrahim, N.A.; Zainuddin, N.; Yunus, W.M.; Hassan, H.A. Mechanical, Thermal and Morphological Properties of Poly(lactic acid)/Epoxidized Palm Olein Blend, *Molecules*. *Molecules* **2012**, *17*, 11729–11747. [[CrossRef](#)] [[PubMed](#)]
43. Lascano, D.; Quilies-Carrillo, L.; Balart, R.; Boronat, T.; Montanes, N. Toughened Poly(Lactic acid)-PLA Formulations by Binary Blends with Poly(Butylene Succinate-co-Adipate)-PBSA and Their Shape Memory Behaviour. *Materials* **2019**, *12*, 622. [[CrossRef](#)]
44. Silverajah, V.S.; Ibrahim, N.A.; Yunus, W.M.; Hassan, H.A.; Woei, C.B. A Comparative Study on the Mechanical, Thermal and Morphological Characterization of Poly(lactic acid)/Epoxidized Palm Oil Blend. *Int. J. Mol. Sci.* **2012**, *13*, 5878–5898. [[CrossRef](#)]
45. Ali, F.; Chang, Y.-W.; Kang, S.C.; Yoon, J.Y. Thermal, mechanical and rheological properties of poly(lactic acid)/epoxidized soybean oil blends. *Polym. Bull.* **2009**, *62*, 91–98. [[CrossRef](#)]
46. Pyda, M.; Bopp, R.C.; Wunderlich, B. Heat capacity of poly(lactic acid). *J. Chem. Thermodyn.* **2004**, *36*, 731–742. [[CrossRef](#)]
47. Pan, P.; Inoue, Y. Polymorphism and isomorphism in biodegradable polyesters. *Progr. Polym. Sci.* **2009**, *34*, 605–640. [[CrossRef](#)]
48. Cocca, M.; Androsch, R.; Righetti, M.C.; Malinconico, M.; Di Lorenzo, M.L. Conformationally disordered crystals and their influence on material properties: The cases of isotactic polypropylene, isotactic poly(1-butene), and poly(L-lactic acid). *J. Mol. Struct.* **2014**, *1078*, 114–132. [[CrossRef](#)]
49. Androsch, R.; Schick, C.; Di Lorenzo, M.L. Melting of conformationally disordered crystals  $\alpha'$ -phase of poly(L-lactic acid). *Macromol. Chem. Phys.* **2014**, *215*, 1134–1139. [[CrossRef](#)]
50. Minakov, A.A.; Mordvintsen, D.A.; Schick, C. Melting and reorganization of poly(ethylene terephthalate) on fast heating (1000 K/s). *Polymer* **2004**, *45*, 3755–3763. [[CrossRef](#)]
51. Righetti, M.C.; Laus, M.; Di Lorenzo, M.L. Temperature dependence of the rigid amorphous fraction in poly(ethylene terephthalate). *Eur. Polym. J.* **2014**, *58*, 60–68. [[CrossRef](#)]
52. Sato, K.; Ueno, S.; Yano, J. Molecular interactions and kinetic properties of fats. *Prog. Lipid Res.* **1999**, *38*, 1–116. [[CrossRef](#)]
53. Ferrari, C.; Angiuli, M.; Tombari, E.; Righetti, M.C.; Matteoli, E.; Salvetti, G. Promoting calorimetry for olive oil authentication. *Thermochim. Acta* **2007**, *459*, 58–63. [[CrossRef](#)]
54. Barba, L.; Arrighetti, G.; Calligaris, S. Crystallization and melting properties of extra virgin olive oil studied by synchrotron XRD and DSC. *Eur. J. Lipid. Sci. Technol.* **2013**, *115*, 322–329. [[CrossRef](#)]
55. Bayes-Garcia, L.; Calvet, T.; Cuevas-Diarte, M.A.; Ueno, S. From Trioleoyl glycerol to extra virgin olive oil through multicomponent triacylglycerol mixtures: Crystallization and polymorphic transformation examined with differential scanning calorimetry and X-ray diffraction techniques. *Food Res. Int.* **2017**, *99*, 476–484. [[CrossRef](#)] [[PubMed](#)]
56. Righetti, M.C.; Gazzano, M.; Di Lorenzo, M.L.; Androsch, R. Enthalpy of melting of  $\alpha'$ - and  $\alpha$ -crystals of poly(L-lactic acid). *Eur. Polym. J.* **2015**, *70*, 215–220. [[CrossRef](#)]
57. Saeidlou, S.; Huneault, M.A.; Li, H.; Park, C.B. Poly(lactic acid) crystallization. *Progr. Polym. Sci.* **2012**, *37*, 1657–1677. [[CrossRef](#)]
58. Androsch, R.; Di Lorenzo, M.L. Crystal Nucleation in Glassy Poly(L-lactic acid). *Macromolecules* **2013**, *46*, 6048–6056. [[CrossRef](#)]
59. Di Lorenzo, M.L.; Androsch, R. Stability and Reorganization of  $\alpha'$ -Crystals in Random L/D-Lactide Copolymers. *Macromol. Chem. Phys.* **2016**, *217*, 1534–1538. [[CrossRef](#)]
60. Baiardo, M.; Frisoni, G.; Scandola, M.; Rimelen, M.; Lips, D.; Ruffieux, K.; Wintermantel, E. Thermal and mechanical properties of plasticized poly(L-lactic acid). *J. Appl. Polym. Sci.* **2003**, *90*, 1731–1738. [[CrossRef](#)]
61. Jacobsen, S.; Fritz, H.G. Plasticizing polylactide—The effect of different plasticizers on the mechanical properties. *Polym. Eng. Sci.* **1999**, *39*, 1303–1310. [[CrossRef](#)]
62. Barnes, H.A.; Hutton, J.F.; Walters, K. *An Introduction to Rheology*, 1st ed.; Elsevier Science: Amsterdam, The Netherlands, 1989.
63. Dorgan, J.R. Rheology of poly(lactic acid). In *Poly(lactic acid): Synthesis, Properties, Processing, and Applications*; Auras, R., Lim, L.-T., Selke, S.E.M., Tsuji, H., Eds.; John Wiley & Sons: Hoboken, NJ, USA, 2010; pp. 125–139.

64. Palade, L.-I.; Lehermeier, H.J.; Dorgan, J.R. Melt Rheology of High L-Content Poly (lactic acid). *Macromolecules* **2001**, *34*, 1384–1390. [[CrossRef](#)]
65. Domenek, S.; Fernandes-Nassar, S.; Ducruet, V. Rheology, Mechanical Properties, and Barrier Properties of Poly(lactic acid). *Adv. Polym. Sci.* **2017**, *279*, 303–342. [[CrossRef](#)]
66. Wang, N.; Zhang, X.; Ma, X.; Fang, J. Influence of carbon black on the properties of plasticized poly(lactic acid) composites. *Polym. Degrad. Stab.* **2008**, *93*, 1044–1052. [[CrossRef](#)]
67. Cocca, M.; Di Lorenzo, L.; Maliconico, M.; Frezza, V. Influence of crystal polymorphism on mechanical and barrier properties of poly(L-lactic acid). *Eur. Polym. J.* **2011**, *47*, 1073–1080. [[CrossRef](#)]
68. Wasanasuk, K.; Tashiro, K. Theoretical and Experimental Evaluation of Crystalline Moduli of Various Crystalline Forms of Poly(L-lactic acid). *Macromolecules* **2012**, *45*, 7019–7026. [[CrossRef](#)]



© 2019 by the authors. Licensee MDPI, Basel, Switzerland. This article is an open access article distributed under the terms and conditions of the Creative Commons Attribution (CC BY) license (<http://creativecommons.org/licenses/by/4.0/>).